

Investigation of the obscuring circumnuclear torus in the active galaxy Mrk231

Hans-Rainer Klöckner^{1,2}, Willem A. Baan² and Michael A. Garrett³

1. Kapteyn Astronomical Institute, University of Groningen, 9700 AV, Groningen, The Netherlands
2. ASTRON, P.O.Box 2, 7990 AA, Dwingeloo, The Netherlands
3. JIVE, Joint Institute for VLBI in Europe, PO Box 2, 7990 AA Dwingeloo, The Netherlands

published in Nature Vol. 421, 821–823, 20 February 2003

Active galaxies are characterized by prominent emission from their nuclei. In the unified view of active galaxies, the accretion of material onto a massive compact object - now generally believed to be a black hole - provides the fundamental power source (Rees, 1984). Obscuring material along the line of sight can account for the observed differences in nuclear emission (Krolik & Begelman, 1988; Krolik, 1999), which determine the classification of AGN (for example, as Seyfert 1 or Seyfert 2 galaxies). Although the physical processes of accretion have been confirmed observationally (Greenhill et al., 1995; Gallimore et al., 1997), the structure and extent of the obscuring material have not been determined. Here we report observations of powerful hydroxyl (OH) line emissions that trace this obscuring material within the circumnuclear environment of the galaxy Markarian 231. The hydroxyl (mega)-maser emission shows the characteristics of a rotating, dusty, molecular torus (or thick disk) located between 30 and 100 pc from the central engine. We now have a clear view of the physical conditions, the kinematics and the spatial structure of this material on intermediate size scales, confirming the main tenets of unification models.

Observations of powerful molecular water-vapour and hydroxyl megamaser emissions, which are a million times more luminous than their galactic counterparts (Baan, 1985), have provided unique information about distinct regions within galactic nuclei. Water-vapour masers can map out the central few parsecs of an AGN, tracing the rotation of nuclear accretion disks and the state of molecular material surrounding the radio jets (Maloney, 2002). The inferred geometry and thickness of these disks, however, cannot account for the observed obscuration signature and the radiation patterns seen in active

galactic nuclei (AGN) (Maloney, 2002; Herrnstein et al., 1998). On the other hand, the hydroxyl masers in galactic nuclei are spread across hundreds of parsecs (Diamond et al., 1999; Lonsdale et al., 1998; Pihlström et al., 2001). Their tight correlation with the infrared emission (Baan, 1989) indicates a strong association with the dusty obscuring material along the line of sight towards the nucleus (Krolik & Begelman, 1988; Krolik, 1999). To study the distribution of the hydroxyl megamaser emission with respect to the nuclear engine at a resolution of tens of parsecs in Mrk 231, we performed very-long-baseline interferometry (VLBI) radio observations with the European VLBI Network (EVN). Mrk 231 is the most luminous infrared galaxy in the local universe (distance of 172 Mpc), and is undergoing a merger as indicated by the high dust content and the prominent tidal tails observed at optical wavelengths. The nuclear power source has been classified (Baan et al., 1998) as a Seyfert 1, which in the unification scheme would suggest that the observer has a direct, and almost unobscured, line-of-sight view into the broad-line emission region at parsec scales. The location of the nuclear engine on similar scale sizes is traced by the radio outflow (Ulvestad et al., 1999b), which extends to almost a hundred parsecs (Ulvestad et al., 1999a).

The EVN data reveal an OH emission structure with an east-west extent of 130 pc that is straddling a north-south elongated radio continuum emission (Fig. 1). This continuum emission has been further resolved into a lobe-core-lobe structure (Ulvestad et al., 1999a) of 80 pc at position angle $PA = 8^\circ$, which is found to be misaligned by 57° with the core radio structure on parsec scales (Ulvestad et al., 1999b). The emission spectrum integrated across the whole OH emitting region displays the two main hydroxyl lines at 1667 and 1665 MHz showing a line-width of around 200 km s^{-1} (full-width at half-maximum, FWHM) at a centroid velocity of 12610 km s^{-1} (Fig. 2). The EVN data and also the intermediate-scale MERLIN (Richards et al., 2000) observations account for only half of the integrated line emission seen by the Westerbork Synthesis Radio Telescope (WSRT; see Figure 2) and previous single-dish measurements (Baan, 1985). This missing emission component must therefore originate within the resolution gap between the EVN and WSRT observations, in an extended region between 190 pc and 11 kpc of the nucleus. This component is probably associated with the nuclear continuum emission (Taylor et al., 1999) and the CO(1-0) line emission (Bryant & Scoville, 1996; Downes & Solomon, 1998). Figure 3 (top panel) presents the spatial velocity distribution, which is similar for each of the two hydroxyl lines and which has

an overall velocity shift of about 160 km s^{-1} from the northwest towards the southeast. The velocity width of the emission lines has an average value of about 70 km s^{-1} (FWHM) across the northern part of the radio continuum emission. On the other hand, there is also a distinct OH emission region at the northwestern edge of the continuum emission that has a velocity similar to that seen towards the centre of the radio core, and which has a distinctly higher velocity width of 85 km s^{-1} (Figure 3; middle panel).

The nature of the OH emission observed in the nucleus of Mrk 231 adds a new component to the hierarchical structure of this system, and complements the information obtained with other tracers at lower resolution. We find that the OH velocity field with its symmetry axis at $\text{PA} = 34^\circ$ does not agree with that of the kiloparsec-scale CO(1-0) structure (Bryant & Scoville, 1996; Downes & Solomon, 1998) having a $\text{PA} = 0^\circ$. Neither does it agree with the large-scale radio outflow ($\text{PA} = 8^\circ$), or the more compact CO(2-1) distribution (Downes & Solomon, 1998) extending up to 850 pc at $\text{PA} = 18^\circ$. However, the OH velocity field is in agreement with that of the line-of-sight HI absorption (Carilli et al., 1998) at $\text{PA} = 27^\circ$. The HI absorption is detected against a diffuse radio-emitting halo with an extent of about 350 pc and an orientation of $\text{PA} = 22^\circ$. This diffuse radio halo, which is possibly associated with a circumnuclear starburst (Taylor et al., 1999), could then also trace the dense and opaque interstellar medium of a disk or torus (Carilli et al., 1998) inclined at 56° . The integrated HI velocity dispersion (Carilli et al., 1998) of $193 \pm 25 \text{ km s}^{-1}$ agrees well with that of the hydroxyl lines (Fig. 2). This suggests that the OH emission indeed originates in the central regions of a circumnuclear rotating disk or torus having an outer structure that is traced by the CO(2-1) emission.

The energy source responsible for the excitation of the OH molecules is the extreme far-infrared radiation (Baan, 1989) field in Mrk 231. The observed far-infrared spectral temperature of around 43 K provides the ideal pumping conditions for the OH clouds, which could range in size from 10 pc up to 100 pc (Henkel et al., 1987; Randell et al., 1995). The ratio of the intensity of the two maser lines varies rather smoothly across the entire emission structure and has an average value of 1.8, as expected for local temperature equilibrium (LTE). This would indicate that the observed emission lines are optically thin and are mostly unsaturated masers. Assuming that the diffuse radio continuum, which serves as a background for the nuclear HI absorption, also serves as a background for the observed OH masers, this emission could

be explained in terms of exponential amplification with a maximal gain of about 2.2 within classical OH maser–models (Baan et al., 1982; Baan, 1985). However, extreme values for the line ratio have been found in the discrepant northwestern region discussed earlier in this text. This region must have a completely different pumping environment than the rest of the structure. The unusual blue–shifted velocity, the slightly higher velocity dispersion, and the line ratios of this discrepant region are all consistent with the theoretically predictions (Baan, 1985; Randell et al., 1995; Wada & Norman, 2002; Baan, 1985) for an interaction region between the radio outflow and the molecular environment.

The molecular environment described above for the nuclear region of Mrk 231 is very similar to the dust structures found in active galaxies such as NGC 4261 using the Hubble Space Telescope (van Langevelde et al., 2000). We have applied an axisymmetric torus model with a circular cross–section to the EVN data, in order to determine the structural boundaries in the nuclear region. The compact molecular structure surrounding the nucleus is misaligned with the large–scale molecular disk of the galaxy by 34° . The radius of the inner cavity of the torus would be about 30 pc, as suggested by the location of the northwestern interaction region. The outer edge of the torus spans a diameter of 200 pc, which is based on the 4 mJy contours of the diffuse radio emission (Carilli et al., 1998) and on far–infrared blackbody estimates (Downes & Solomon, 1998). This region also serves as a radio background for the OH amplification process. These parameters result in a torus structure with a radius of 65 pc and a thickness of 70 pc, which accounts for an obscuration angle of 60° centered on the plane of the torus and which is representative of values found for other galaxies (Schmitt et al., 2001). The orientation and the shape of the extended radio contours and the symmetry axis of the velocity field indicate that the torus is tilted upward from the line of sight by 56° , and is rotated anticlockwise by 35° . This inferred model for the torus has been displayed as a wire–structure representation and is presented in Figure 3 (bottom panel). The nuclear radiation cones with opening angles of 60° , assumed to be similar to those seen in M 87 (Junor et al., 1999), represent the directions with an unobscured view of the nucleus. The radio outflow follows a twisted path within these cones, starting at the nucleus (at PA = 65°) and ending up as a double source aligned with the symmetry axis of the outer disk (at PA = 8°) (Ulvestad et al., 1999b,a). As a result, this parameterization indicates that the nuclear accretion disk,

that collimates the jet outflow inside the central cavity, is actually misaligned by 30° with the plane of the molecular torus.

In reality, the proposed torus structure does not need to have a circular cross-section. In addition, it will most probably be wrapped inside a cocoon-like surface region with a higher temperature, and will have the same outer extent of 460 pc as the diffuse radio emission and the HI absorbing gas (Carilli et al., 1998). However, the representation of the inner part of this rotating dusty and molecular torus in Mrk 231 is consistent with (all) current models of galactic nuclei and theoretical investigations (Krolik, 1999), and supports the unification schemes for AGN. Whether a different orientation of the torus and the nuclear accretion disk represents a special case or is a general characteristic of active nuclei needs to be investigated with VLBI observations of other megamaser galaxies hosting a similar nuclear power source.

Acknowledgments

We thank C. Carilli for providing a map of the diffuse continuum structure in Mrk 231. H.-R.K thanks O. Möller for advice on programming in OpenGL software. The European VLBI Network is a joint facility of European, South African, and Chinese radio astronomy institutes funded by their national research councils. The Westerbork Synthesis Radio Telescope is operated by the ASTRON (Netherlands Foundation for Research in Astronomy) with support from the Netherlands Foundation for Scientific Research NWO.

Correspondence and requests for material should be addressed to H.-R. K. (e-mail: hrkloeck@astro.rug.nl).

References

- Baan W.A.: 1985, *Nat* 315, 26
- Baan W.A.: 1989, *ApJ* 338, 804
- Baan W.A., Salzer J.J., Lewinter R.D.: 1998, *ApJ* 509, 633
- Baan W.A., Wood P.A.D., Haschick A.D.: 1982, *ApJ Lett.* 260, L49
- Bryant P.M., Scoville N.Z.: 1996, *ApJ* 457, 678

- Carilli C.L., Wrobel J.M., Ulvestad J.S.: 1998, *AJ* 115, 928
- Diamond P.J., Lonsdale C.J., Lonsdale C.J., Smith H.E.: 1999, *ApJ* 511, 178
- Downes D., Solomon P.M.: 1998, *ApJ* 507, 615
- Gallimore J.F., Baum S.A., O’Dea C.P.: 1997, *Nat* 388, 852
- Greenhill L.J., Jiang D.R., Moran J.M., et al.: 1995, *ApJ* 440, 619+
- Henkel C., Guesten R., Baan W.A.: 1987, *A&A* 185, 14
- Herrnstein J.R., Moran J.M., Greenhill L.J., Blackman E.G., Diamond P.J.: 1998, *ApJ* 508, 243
- Junor W., Biretta J.A., Livio M.: 1999, *Nat* 401, 891
- Krolik J.H.: 1999, Active galactic nuclei : from the central black hole to the galactic environment. Active galactic nuclei : from the central black hole to the galactic environment /Julian H. Krolik. Princeton, N. J. : Princeton University Press, c1999.
- Krolik J.H., Begelman M.C.: 1988, *ApJ* 329, 702
- Lonsdale C.J., Lonsdale C.J., Diamond P.J., Smith H.E.: 1998, *ApJ Lett.* 493, L13
- Maloney P.R.: 2002, *Publications of the Astronomical Society of Australia* 19, 401
- Pihlström Y.M., Conway J.E., Booth R.S., Diamond P.J., Polatidis A.G.: 2001, *A&A* 377, 413
- Randell J., Field D., Jones K.N., Yates J.A., Gray M.D.: 1995, *A&A* 300, 659
- Rees M.J.: 1984, *ARA&A* 22, 471
- Richards A., Cohen, Cole, et al.: 2000, In: Galaxies and their Constituents at Highest Angular Resolution *IAU Symposium*, vol. 205, Astronomical Society of the Pacific, San Francisco, c2001.

Schmitt H.R., Antonucci R.R.J., Ulvestad J.S., et al.: 2001, *ApJ* 555, 663
Taylor G.B., Silver C.S., Ulvestad J.S., Carilli C.L.: 1999, *ApJ* 519, 185
Ulvestad J.S., Wrobel J.M., Carilli C.L.: 1999a, *ApJ* 516, 127
Ulvestad J.S., Wrobel J.M., Roy A.L., et al.: 1999b, *ApJ Lett.* 517, L81
van Langevelde H.J., Pihlström Y.M., Conway J.E., Jaffe W., Schilizzi R.T.:
2000, *A&A* 354, L45
Wada K., Norman C.A.: 2002, *ApJ Lett.* 566, L21

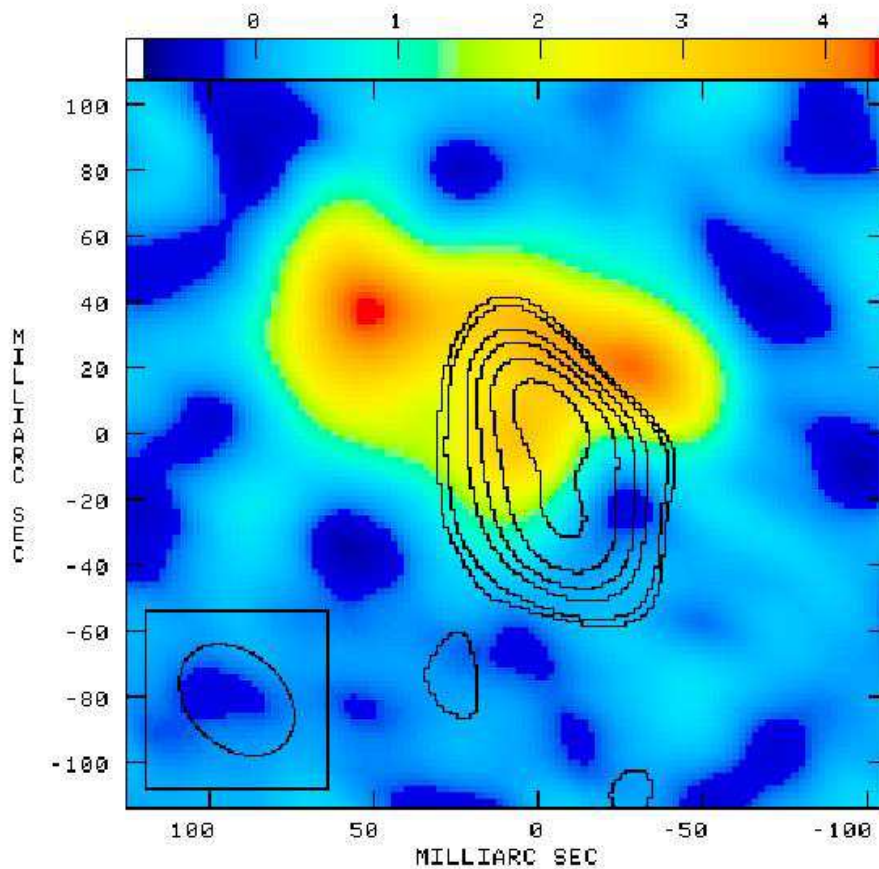


Figure 1: **Hydroxyl and radio-continuum emission in the nucleus of Mrk 231.**

The integrated OH-line emission in pseudo-color (in mJy per beam) is superimposed on the nuclear continuum emission in contours (peak 39 mJy per beam). The contour levels are a geometric progression in factors of the square root of 2 starting at 4 mJy per beam. These EVN observations of Mrk 231 were made on September 1999 for 12 hrs in dual-polarization phase-referencing mode at 1599 MHz and with 256 spectral channels across a total bandwidth of 8 MHz. The synthesized beam is $39 \text{ mas} \times 28 \text{ mas}$, where 1 mas corresponds to a size of 0.83 pc at the distance of Mrk 231 (172 Mpc by assuming $q_0=0.5 \text{ km s}^{-1}$ and $H_0=75 \text{ km s}^{-1} \text{ Mpc}^{-1}$). The data has been correlated at the EVN correlator at the Joint Institute for VLBI in Europe (JIVE), and later transferred to the AIPS packages for calibration of the complex visibilities. The integrated line emission image has been obtained by averaging over the velocity range of the OH lines, after subtraction of the radio continuum, obtained by averaging the channels without line emission.

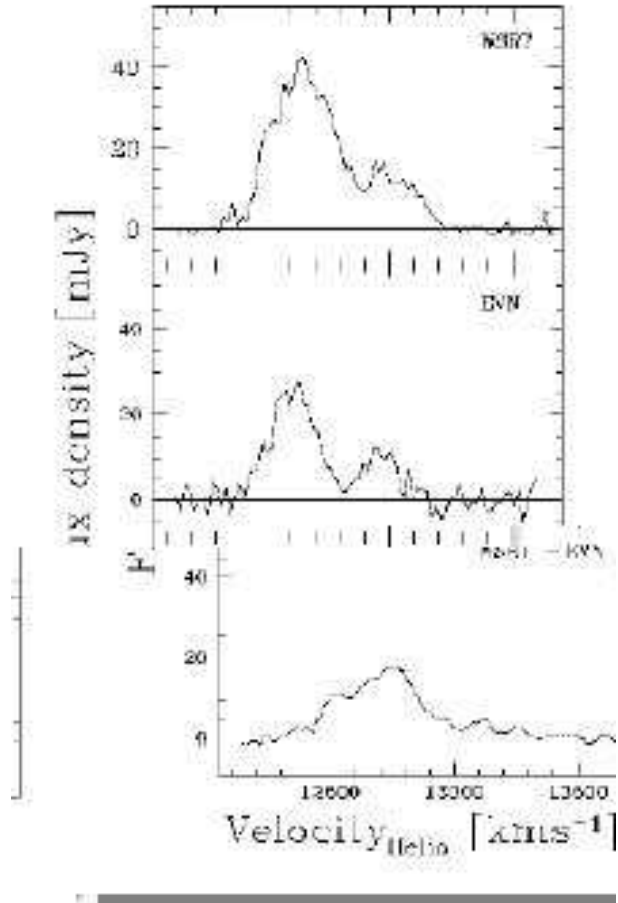


Figure 2: **Hydroxyl emission spectra of Mrk 231 traced at different scale sizes.**

The top panel shows the WSRT spectrum taken at 14 arcsec resolution, the middle panel displays the spectrum for the EVN observations at 39 mas resolution, and the bottom panel displays the difference spectrum of both observations. The emission line features show both OH main lines at 1667 and 1665 MHz that are offset by 365 km s^{-1} ; the velocity scale refers to the 1667 MHz emission line by assuming a heliocentric velocity of $V_{\text{center}} = 12650 \text{ km s}^{-1}$ based on the CO(1-0) centre velocity (Downes & Solomon, 1998). The spectral resolution is 18 km s^{-1} per channel. The OH line width in the EVN data is $214 \pm 11 \text{ km s}^{-1}$ (FWHM), which is 70 km s^{-1} less than for the WSRT data. The residual emission line in the bottom frame counts for 44 % of the OH emission in Mrk 231 and is systematically red-shifted by around 45 km s^{-1} . Similar flux discrepancies, but with no distinct velocity offset, have been found for other OH-MM galaxies studied at high resolution (Diamond et al., 1999; Lonsdale et al., 1998; Pihlström et al., 2001). Similar velocity offsets have also been found for the CO(2-1) emission (Bryant & Scoville, 1996) and the HI absorption in Mrk 231 (Carilli et al., 1998).

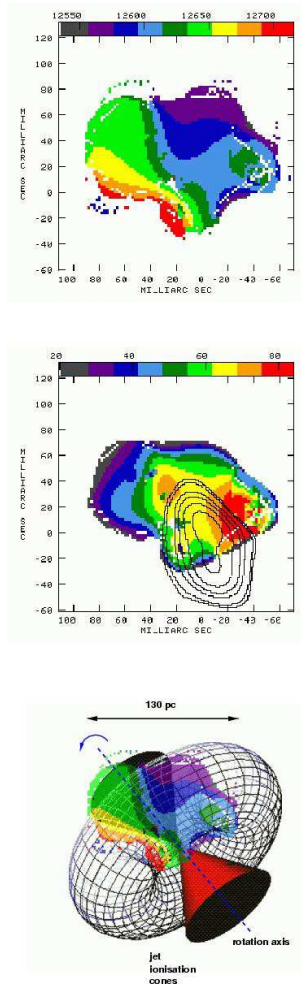


Figure 3: **The circum–nuclear kinematics in Mrk 231.**

Top panel - The velocity field of the OH 1667 MHz emission in the EVN data is shown in pseudo–colors. The spatial resolution is the same as for Fig. 1 and the velocity scale is the same as in Fig. 2. The overall velocity pattern reveals an east–west velocity gradient of 1.41 km s^{-1} per parsec over the entire OH emission such that the northwestern edge of the torus moves towards the observer.

Middle panel - The line width of the 1667 MHz emission lines (in km s^{-1}) is superimposed on the nuclear radio continuum emission in contours displayed in a similar way as in Fig. 1. The diagram shows that the velocity dispersion varies significantly across the emission region. The velocity dispersion structure shows several distinct regions but with the highest values to be found at the western edge of the radio continuum source.

Bottom panel - The inferred model of the nuclear torus in Mrk 231 is displayed as a wire diagram with symmetric ionization cones. This model takes into account all large–scale characteristics of the nuclear radio emission and the OH emission. The symmetry axis of the torus has been inclined upwards by 56° , and then rotated anticlockwise by 35° . The molecular material moves from top–right to bottom–left (northwest to southeast). The virial estimates of the central mass concentration is $7.2 \pm 3.8 \times 10^7 M_\odot$.